BLUE ACTION

The Blue-Action project has received funding from the European Union's Horizon 2020 research and innovation programme under grant agreement No 727852

Decadal predictability of
North Atlantic blocking and the NAO

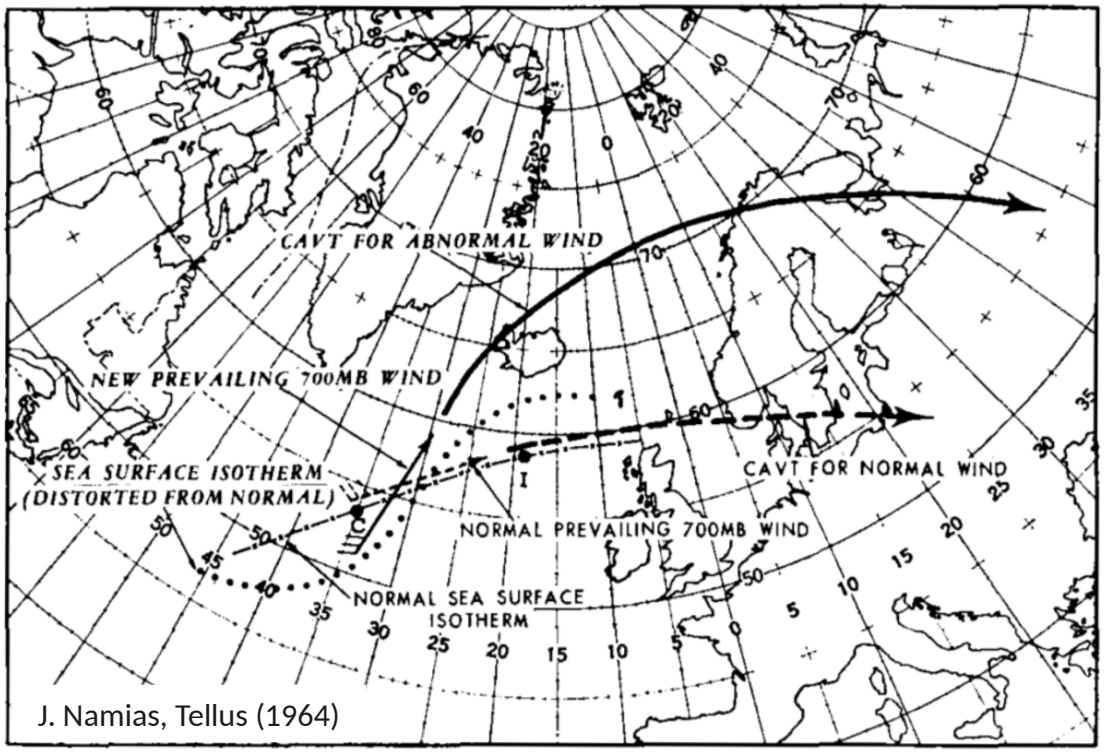

J. Namias, Tellus (1964)

Panos Athanasiadis (CMCC)

Steve Yeager (NCAR), Young-Oh Kwon (WHOI),

Alessio Bellucci & Stefano Tibaldi (CMCC).

panos.athanasiadis@cmcc.it

cmcc
Centro Euro-Mediterraneo sui Cambiamenti Climatici

Why would it be useful to skilfully predict blocking and NAO variability?

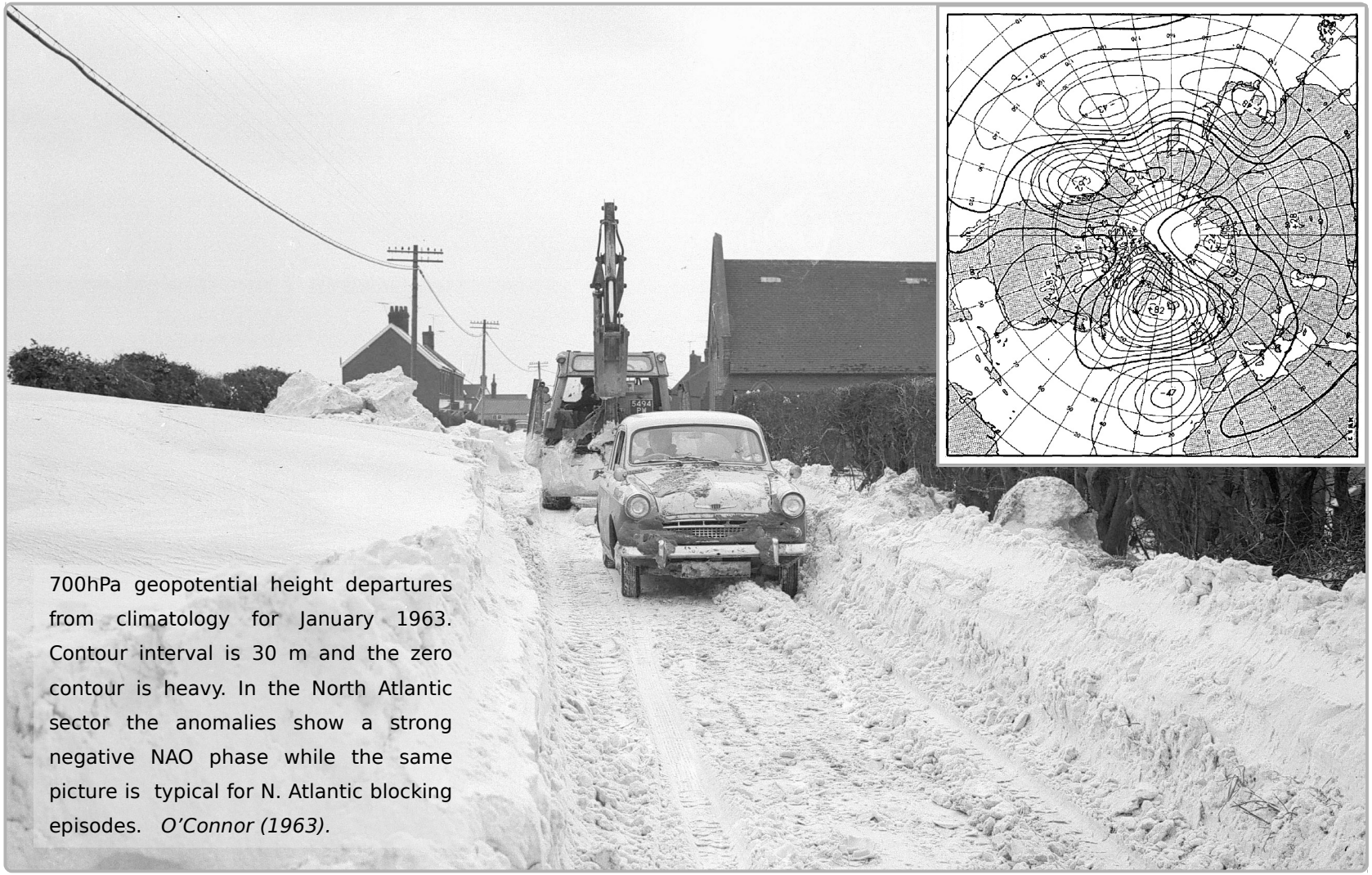

700hPa geopotential height departures from climatology for January 1963. Contour interval is 30 m and the zero contour is heavy. In the North Atlantic sector the anomalies show a strong negative NAO phase while the same picture is typical for N. Atlantic blocking episodes. *O'Connor (1963).*

Greenland Blocking for South Jet.

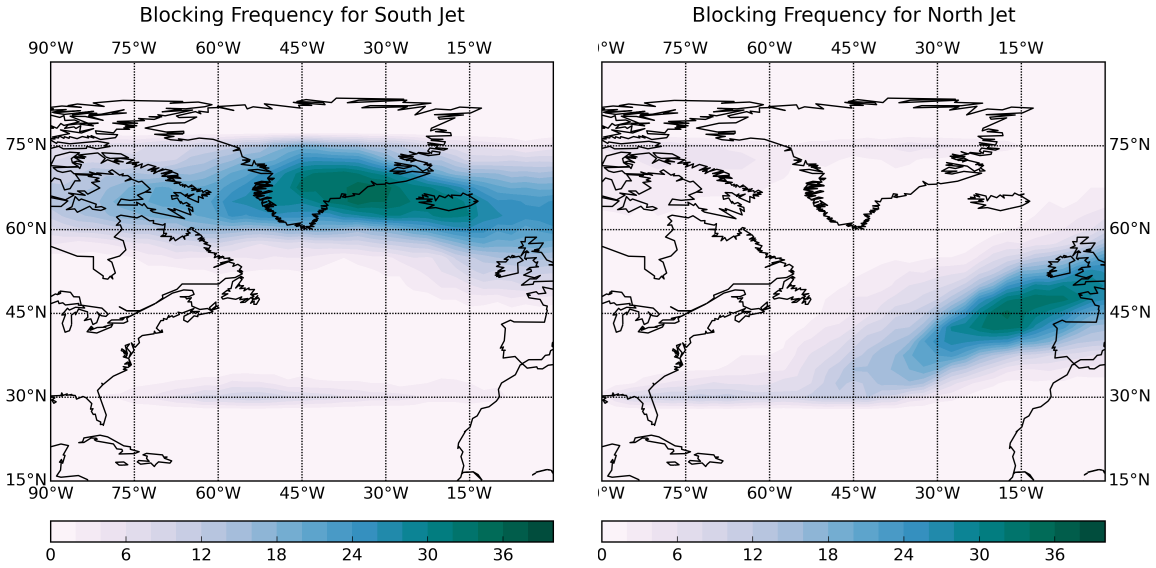

Eastern Atlantic Blocking for North Jet.

Climatological Blocking Frequency (ERA-Interim 1979–2014)

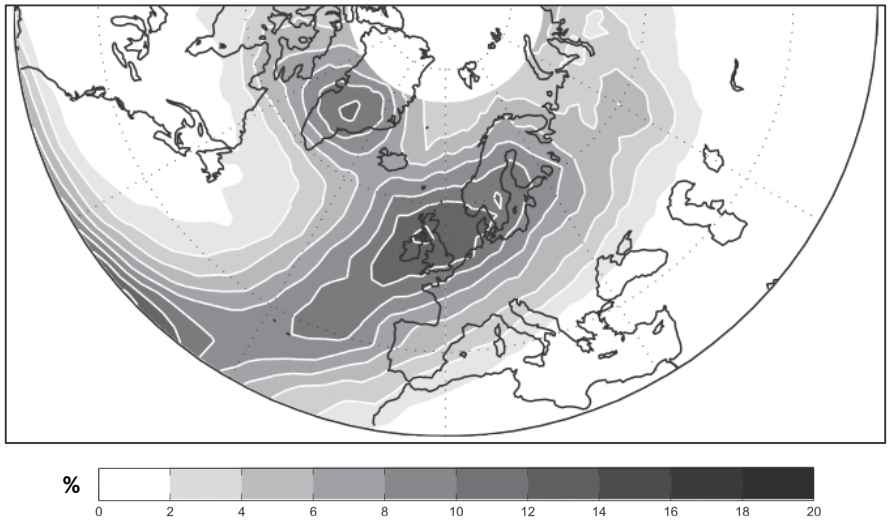

The Euro-Atlantic circulation regimes [Cassou (2008)] and the position of the eddy-driven jet are directly linked to the occurrence of blocking in different parts of the domain.

The NAO+ regime [*Central Jet* in Woollings et al. (2010)] corresponds to the absence of blocking in the domain.

Athanasiadis et al. (2014)

The NAO and blocking exhibit significant predictability at the seasonal timescale.

How about decadal predictions and climate projections?

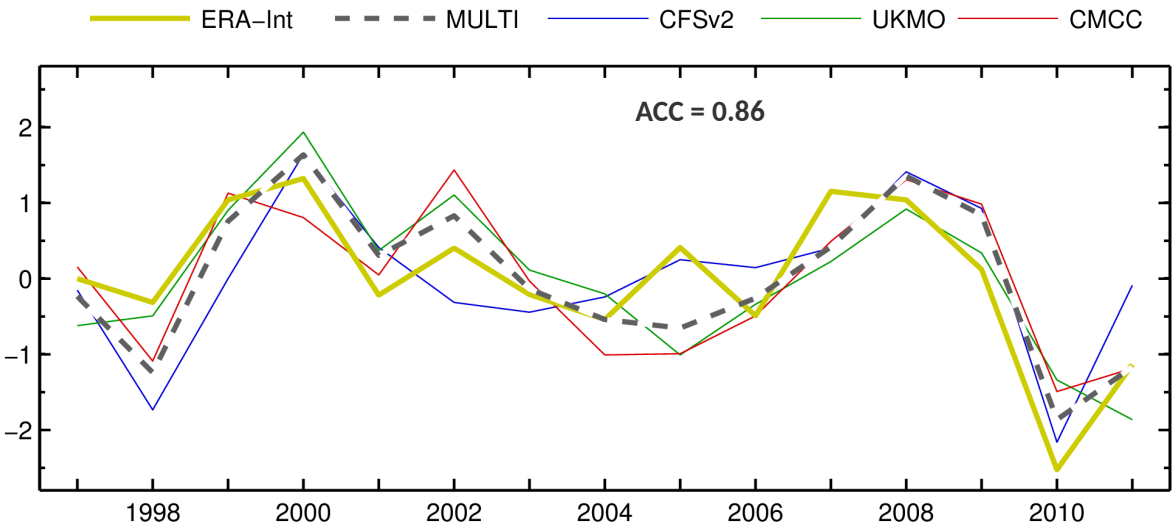

Athanasiadis et al. (2017)

Skill for winter blocking

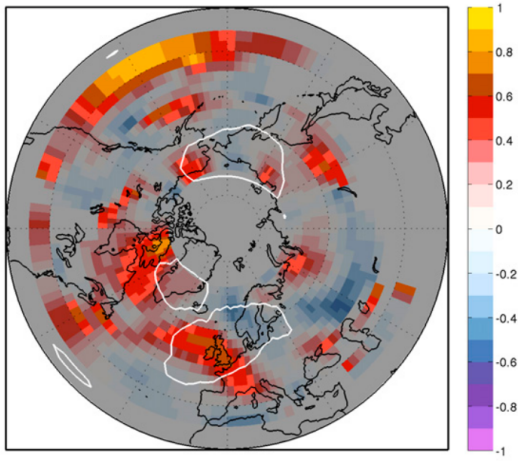

Athanasiadis et al. (2014)

Also: Scaife et al. (2014), Athanasiadis et al. (2014), Riddle et al. (2013)

The blocking statistics are non-stationary.

Over Greenland the frequency varies by a factor of four.

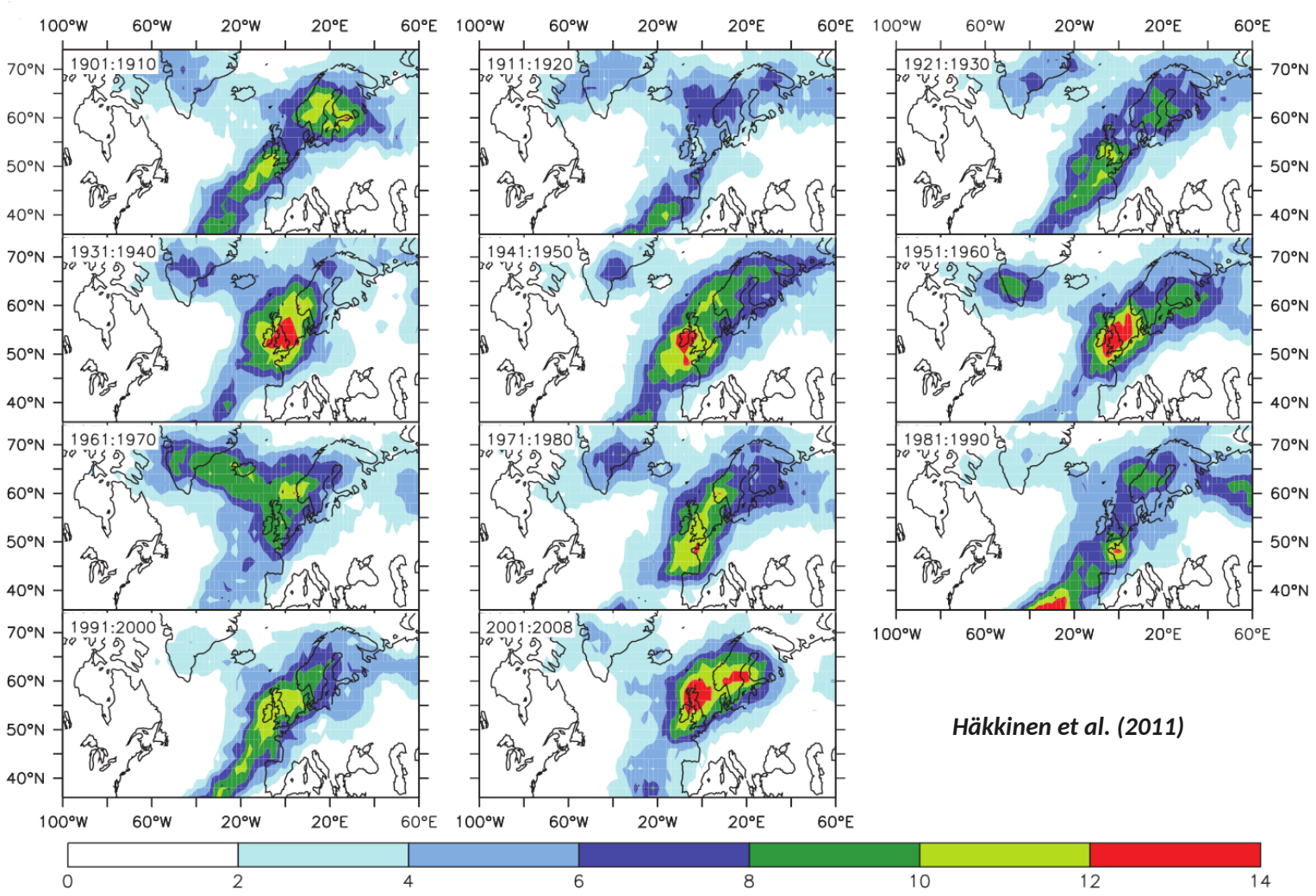

Häkkinen et al. (2011)

Beyond seasonal predictions come near-term climate predictions.

nature climate change

PERSPECTIVE

https://doi.org/10.1038/s41558-018-0359-7

Towards operational predictions of the near-term climate

Yochanan Kushnir[1,25*], Adam A. Scaife[2,3,25*], Raymond Arritt[4,26], Gianpaolo Balsamo[5], George Boer[6], Francisco Doblas-Reyes[7,8], Ed Hawkins[9], Masahide Kimoto[10], Rupa Kumar Kolli[11], Arun Kumar[12], Daniela Matei[13], Katja Matthes[14,15], Wolfgang A. Müller[13,16], Terence O'Kane[17], Judith Perlwitz[18,19], Scott Power[20], Marilyn Raphael[21], Akihiko Shimpo[22], Doug Smith[2], Matthias Tuma[23] and Bo Wu[24]

Near-term climate predictions — which operate on annual to decadal timescales — offer benefits for climate adaptation and resilience, and are thus important for society. Although skilful near-term predictions are now possible, particularly when coupled models are initialized from the current climate state (most importantly from the ocean), several scientific challenges remain, including gaps in understanding and modelling the underlying physical mechanisms. This Perspective discusses how these challenges can be overcome, outlining concrete steps towards the provision of operational near-term climate predictions. Progress in this endeavour will bridge the gap between current seasonal forecasts and century-scale climate change projections, allowing a seamless climate service delivery chain to be established.

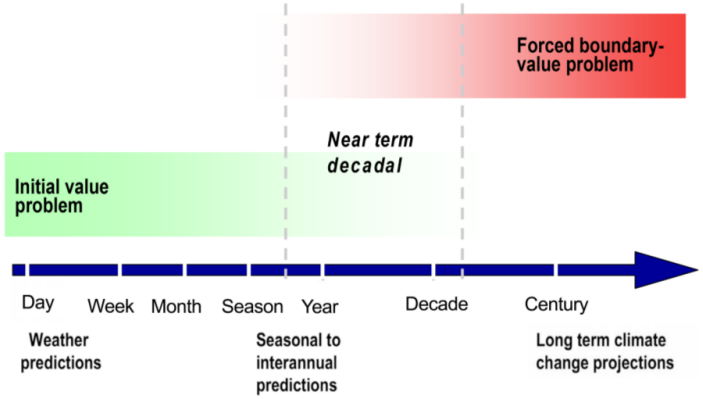

Boer et al. (2016)

Open questions

- If part of the interannual to decadal atmospheric variability in the North Atlantic is driven by the ocean, and given that current decadal hindcasts show high skill in predicting SST anomalies forced by ocean circulation, should not there be some predictability also for the atmosphere?
- For instance, is the occurrence frequency of the dominant Euro-Atlantic circulation regimes (Greenland blocking, Eastern Atlantic blocking and absence of blocking / NAO+) predictable beyond the seasonal timescale?
- If yes, then what are the drivers and the limits of this predictability?
- How many ensemble members are needed?

Data & Methods

- We use a unique data set: NCAR's Decadal Prediction Large Ensemble (CESM-DPLE, 40 members) that allows the atmospheric response to oceanic forcing to emerge from the inherently unpredictable internal atmospheric variability.
- We apply 2D blocking detection to daily Z500 fields from each individual member (62 initialization years: 1954–2015, 10 lead years with 121 days per DJFM season).
- For the NAO, ensemble-mean MSLP monthly-mean fields are used, instead.
- Predictive skill is assessed against the NCEP/NCAR reanalysis (Kalnay et al., 1996) via Anomaly Correlation Coefficient (ACC).
- The statistical significance is thoroughly assessed [Bretherton et al., 1999] accounting for autocorrelation in the timeseries, which reduces the effective sample size. One-sided T-test against the null hypothesis of non-positive correlation.

CESM-DPLE

Community Earth System Model – Decadal Prediction Large Ensemble

Model: Atmosphere Ocean Ice Land	**CESM1.1** CAM5 (1°, 30 levels) POP2 (1°, 60 levels) CICE4 (1°) CLM4
Forcing:	–2005: CMIP5 historical 2006–: CMIP5 RCP 8.5
Initialization: Method Atmosphere Ocean Ice Land	 Full field UI CORE*-forced FOSI CORE*-forced FOSI UI
Ensembles: Ensemble size Start dates	 40 Annual, Nov. 1st 1954–2015 (N=62)
Ensemble generation:	Round-off perturbation of atmospheric initial conditions (only)
Simulation length:	122 months
Uninitialized Ensemble:	40-member CESM 20th century Large Ensemble (Kay et al., 2015)

Blocking detection method in 2D

$$GHGS(\lambda_0, \Phi_0) = \frac{Z500(\lambda_0, \Phi_0) - Z500(\lambda_0, \Phi_S)}{\Phi_0 - \Phi_S},$$

$$GHGN(\lambda_0, \Phi_0) = \frac{Z500(\lambda_0, \Phi_N) - Z500(\lambda_0, \Phi_0)}{\Phi_N - \Phi_0}$$

where Φ_0 ranges from 30°N to 75°N

λ_0 ranges from 0° to 360°

$\Phi_S = \Phi_0 - 15°$, $\Phi_N = \Phi_0 + 15°$.

Instantaneous blocking is identified when:

$GHGS(\lambda_0, \Phi_0) > 0$ and

$GHGN(\lambda_0, \Phi_0) < -10 m/°lat$

Minimum persistence of 5 days.

Scherrer et al. (2006)

Idealized Rex blocking (Z500)

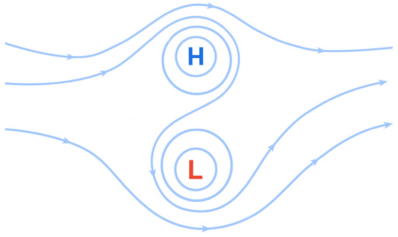

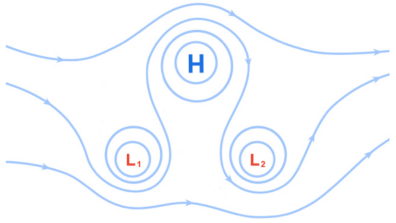

Idealized omega blocking (Z500)

Blocking climatologies (after mean-bias correction for CESM)

For mean-bias correction:
a lead-year dependent daily climatology is subtracted, and the smoothed observed daily climatology is added.

CESM-DPLE (as well as the uninitialized LENS) significantly underestimate the climatological blocking frequency, particularly over Greenland, likely due to underestimating blocking episodes duration.

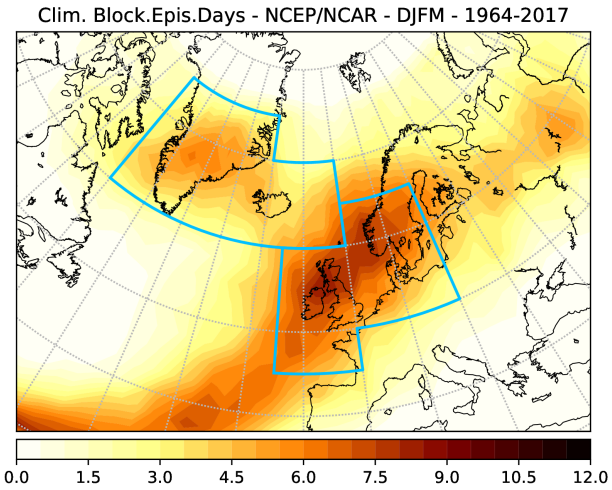

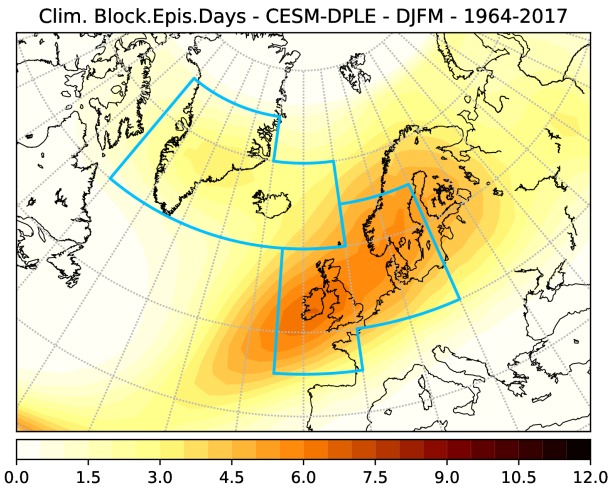

Interannual variability (STD) of blocking frequency

The interannual variability of blocking frequency (a 3-year running average is applied) is proportionally underestimated.

Two areas (Greenland + Iceland: GR-IC, Britain + Scandinavia: BR-SC) are defined linking to known circulation regimes.

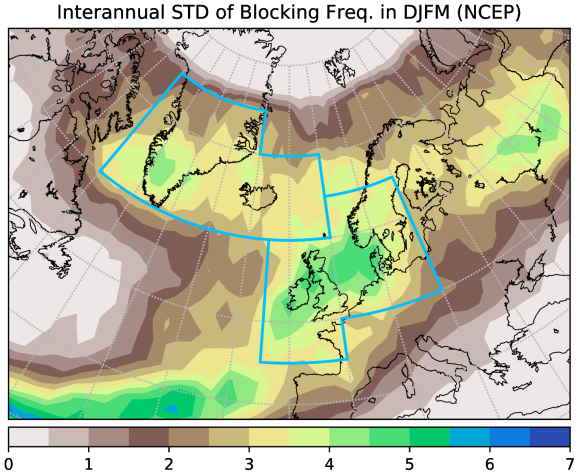

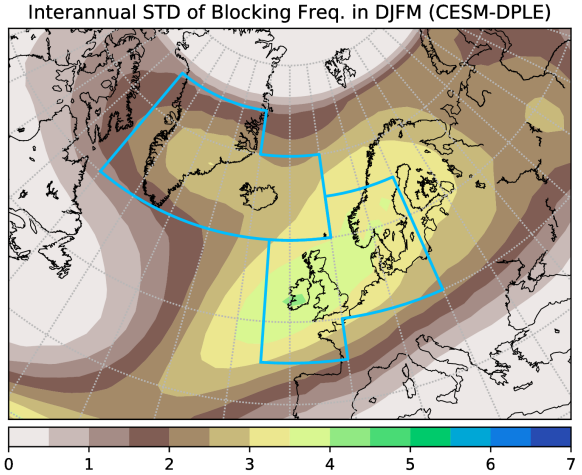

Days per DJFM season

For GR-IC, the skill is highest (ACC=0.58) for the lead-year range 1–8.

For BR-SC, the skill is highest (ACC=0.43) for the lead-year range 6–7.

For both areas and for each lead-year range exhibiting statistically significant skill for the full 40-member ensemble (color lines below, boxes without “o” marker above), the skill increases monotonically with the ensemble size.

The skill does not seem to be saturated for the available ensemble size (40), thus pointing to potential benefits from even larger ensembles.

A multi-system analysis is ongoing.

GREENLAND - ICELAND

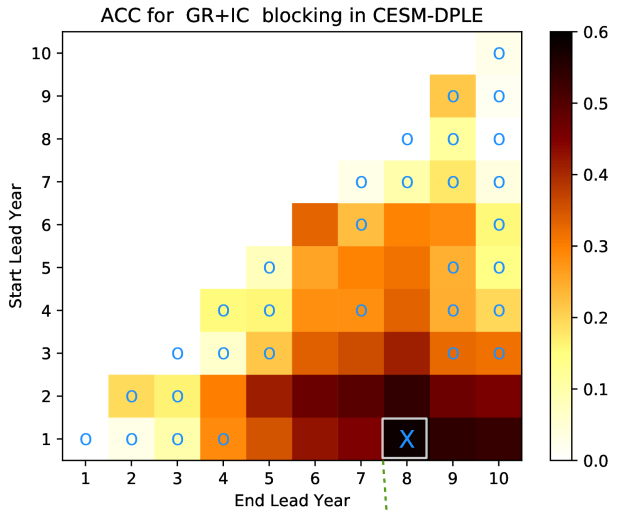

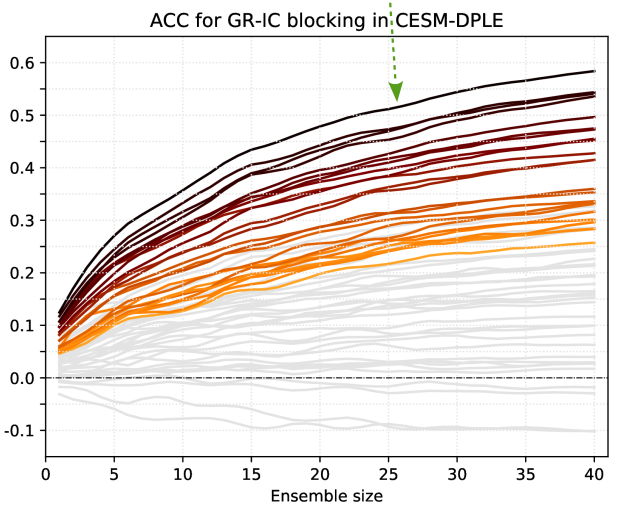

BRITAIN - SCANDINAVIA

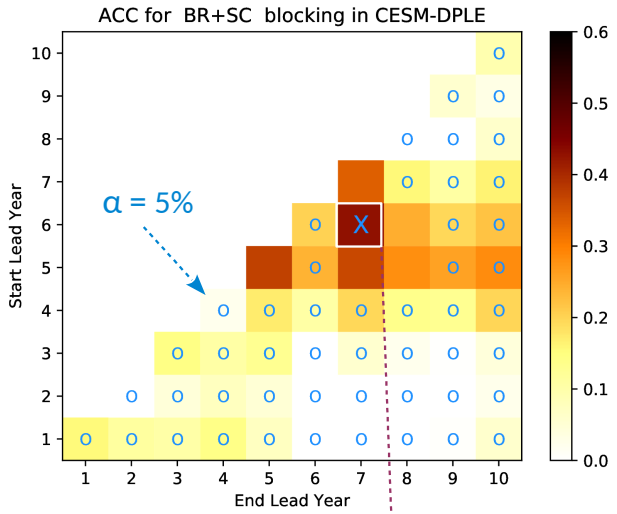

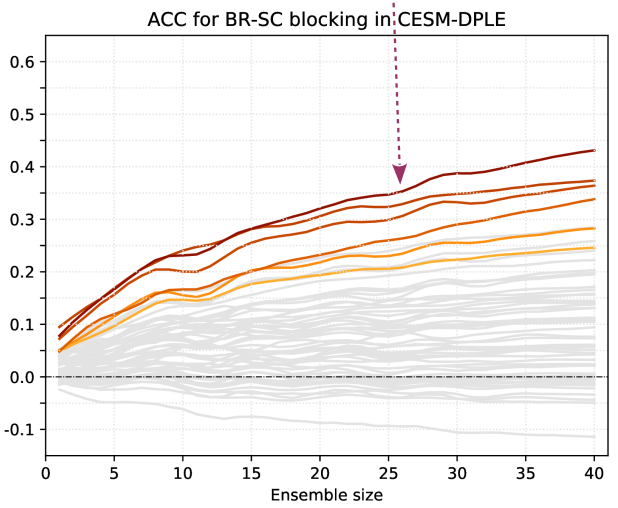

For the lead-year range exhibiting the highest skill for each area, the respective timeseries provide a clue about the frequencies contributing the most to the respective correlation.

Mainly multi-decadal timescales for GR-IC. Inter-decadal to decadal timescales for BR-SC.

Notably, correlations are significantly increased after smoothing the model timeseries.

The respective ACC maps reveal coherent areas of high skill. At each grid point, the number of blocking days per season have been aggregated from the nearest 8 grid points so as to boost statistical significance and reduce noisiness.

GREENLAND - ICELAND

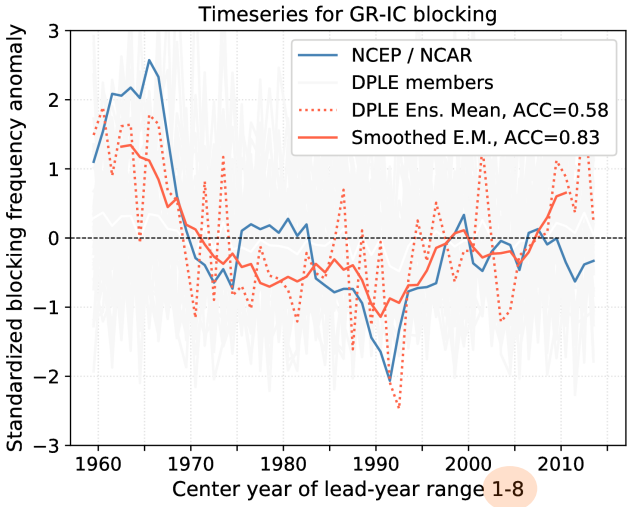

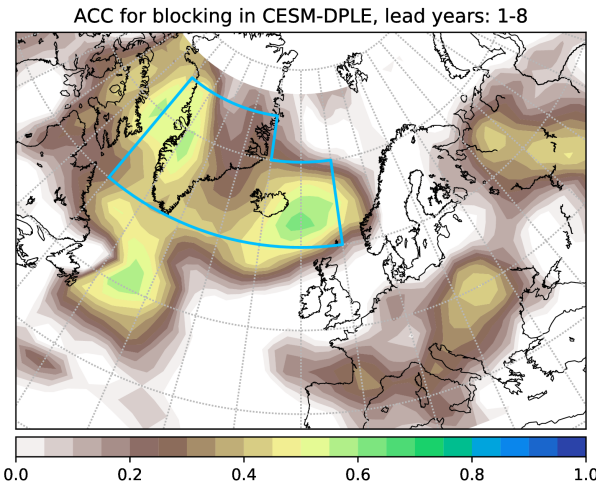

BRITAIN - SCANDINAVIA

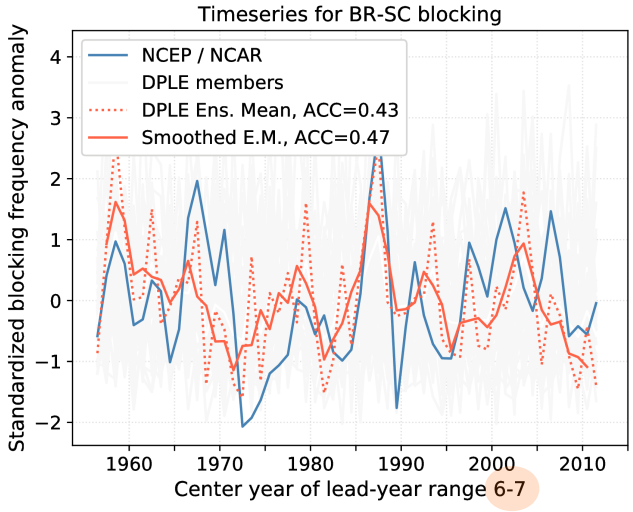

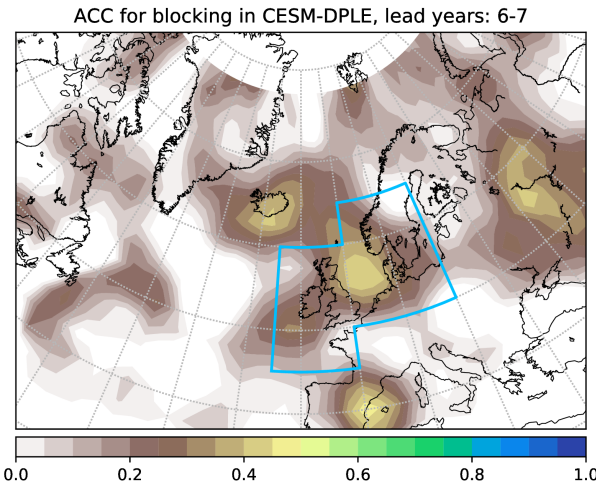

The NAO Index is computed from zonally-averaged MSLP (Jianping and Wang, 2003).

The high skill for GR-IC blocking (0.58) is reflected in equally high skill for the NAO (0.59).

As expected, for the model and the observations alike, the respective timeseries (GR-IC blocking, NAO) exhibit a very high anticorrelation (-0.91).

GREENLAND - ICELAND

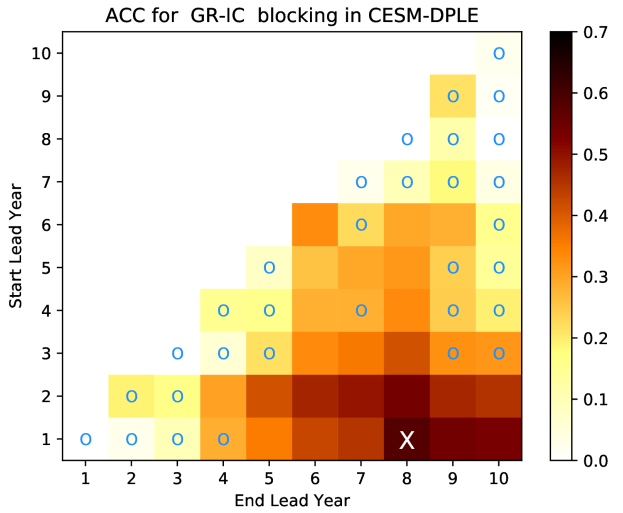

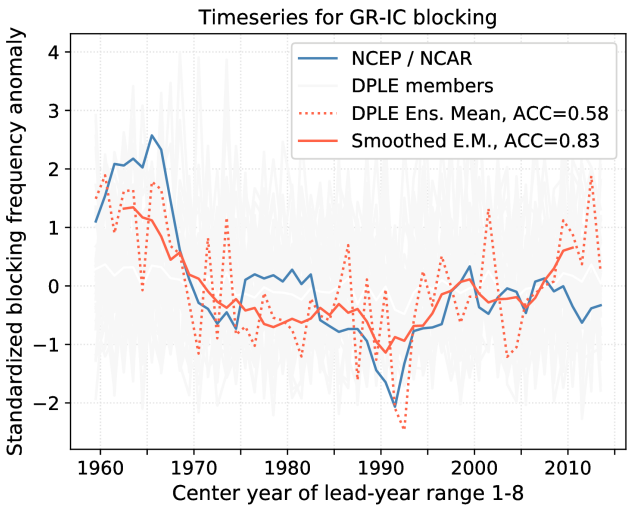

NAO

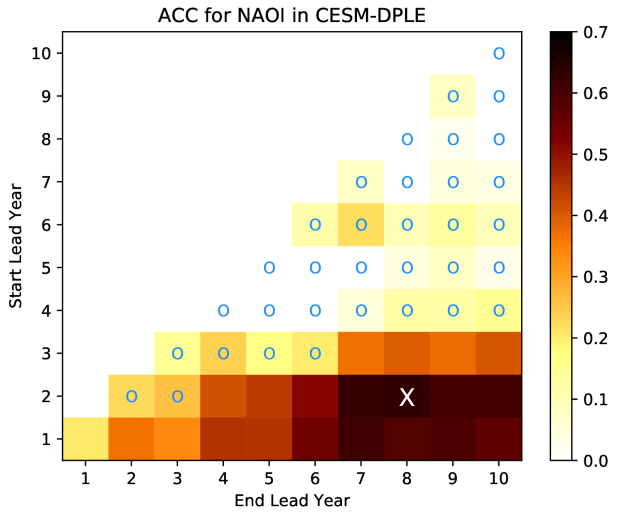

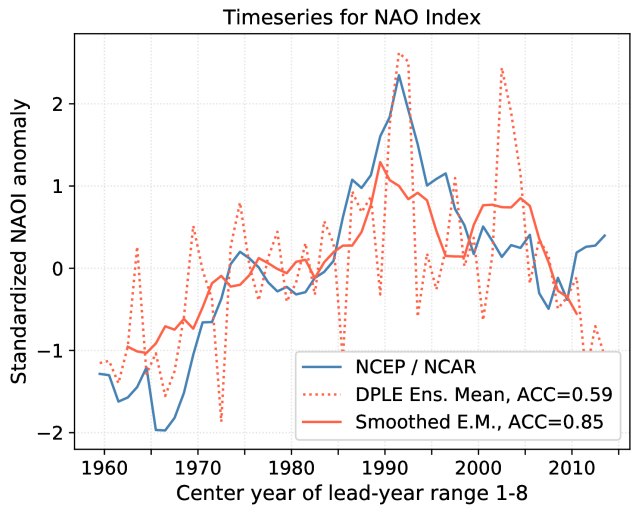

For adfasdfasdfasdf

GREENLAND - ICELAND

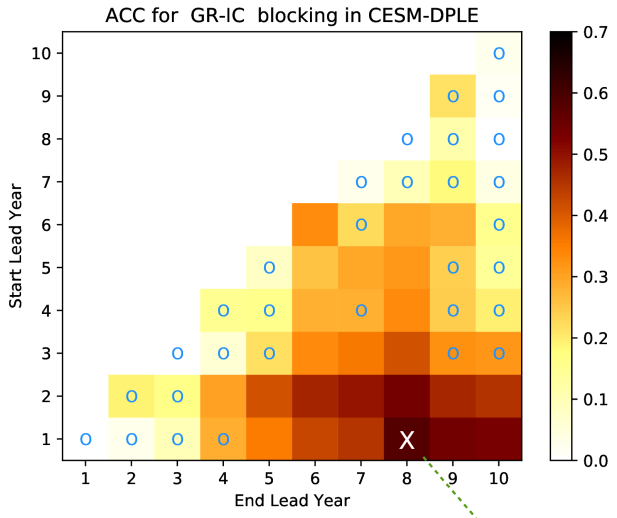

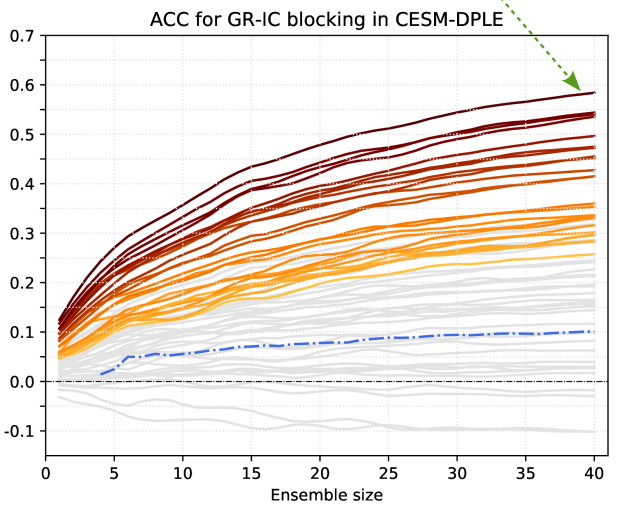

NAO

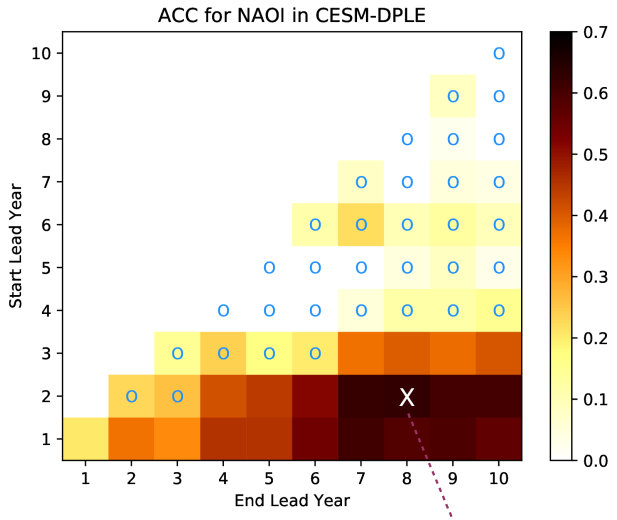

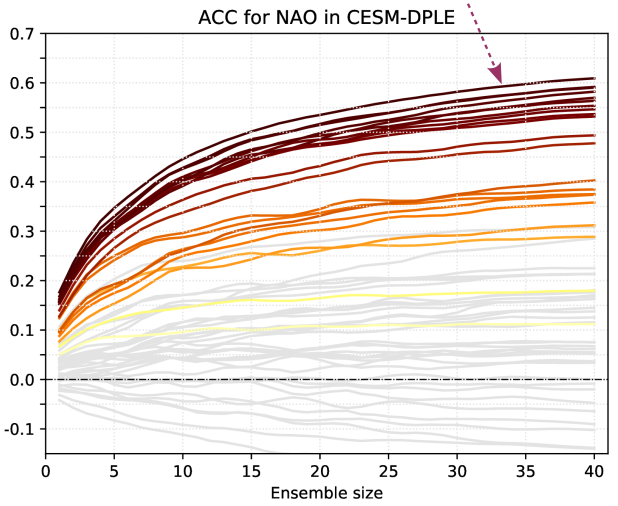

GREENLAND - ICELAND

BRITAIN - SCANDINAVIA

Ensemble-mean SST fields in autumn (SON) are composed on the ensemble-mean blocking frequency in winter (DJFM). Here the respective composite differences are shown for each blocking area.

Strong antisymmetry in the SST anomaly fields was found (results not shown) between *high* and *low* blocking years.

In the lower panels, storminess is found to vary in accordance with the occurrence of blocking.

"T1" refers to "GR-IC"
"T2" refers to "BR-SC"

Pinning down the source of predictability for NAO and blocking is an ongoing effort.

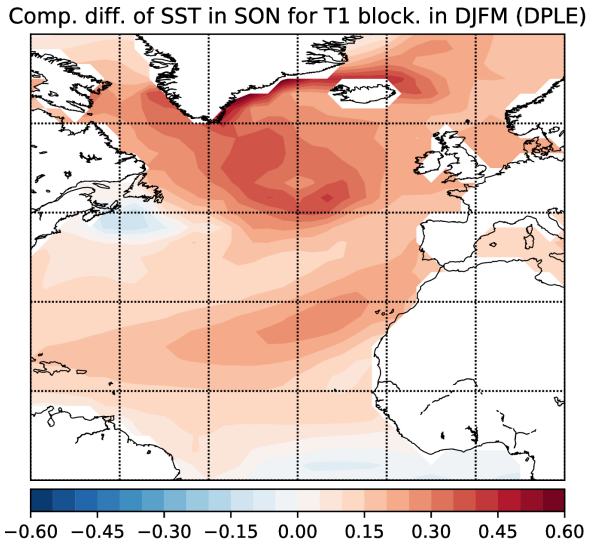

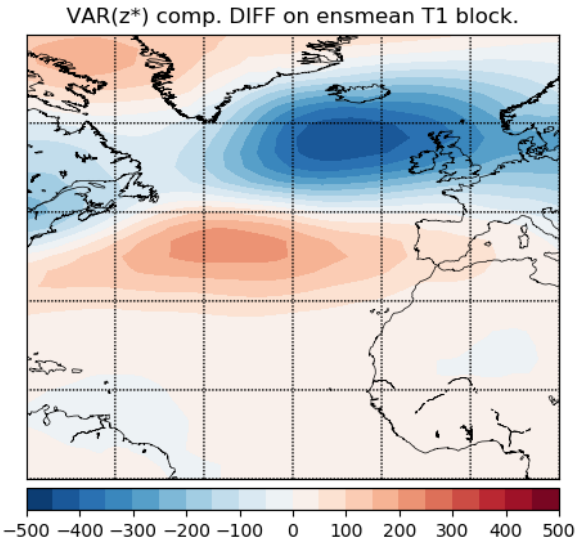

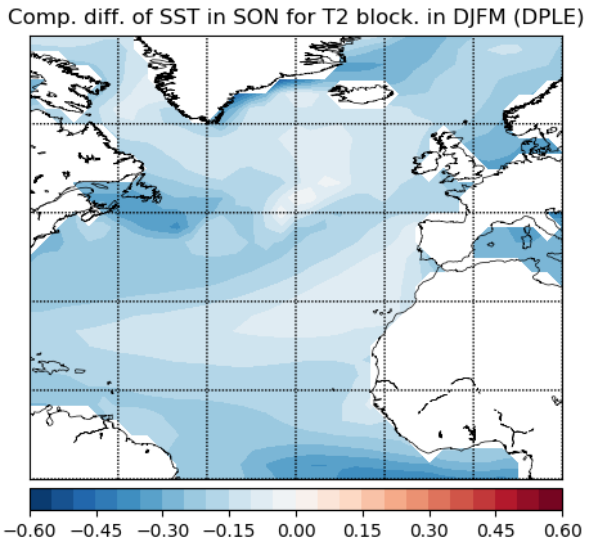

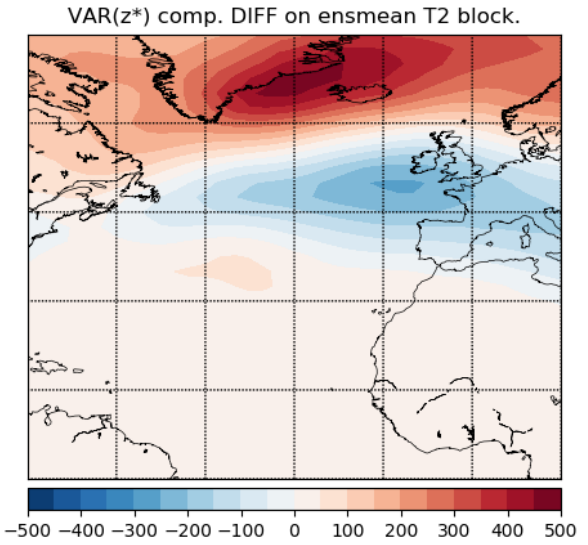

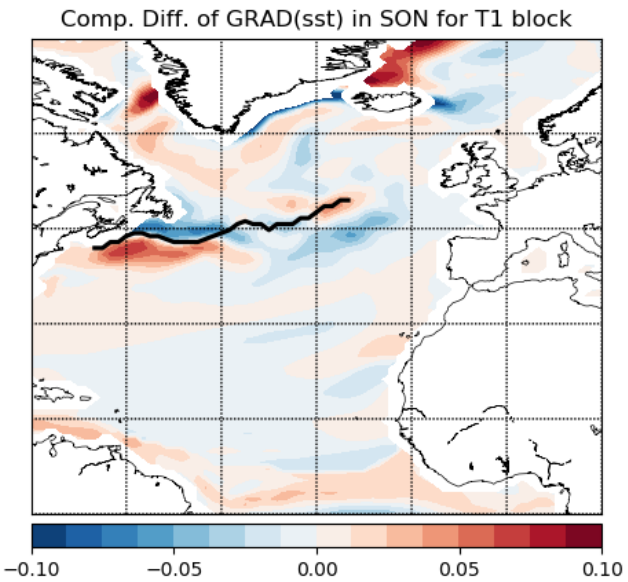

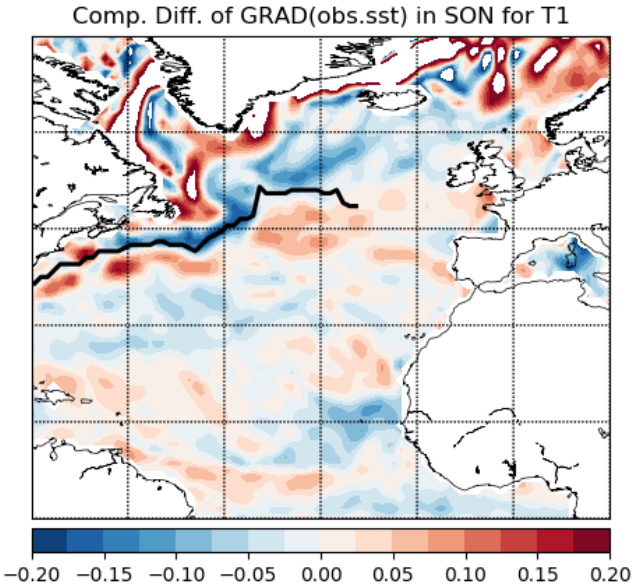

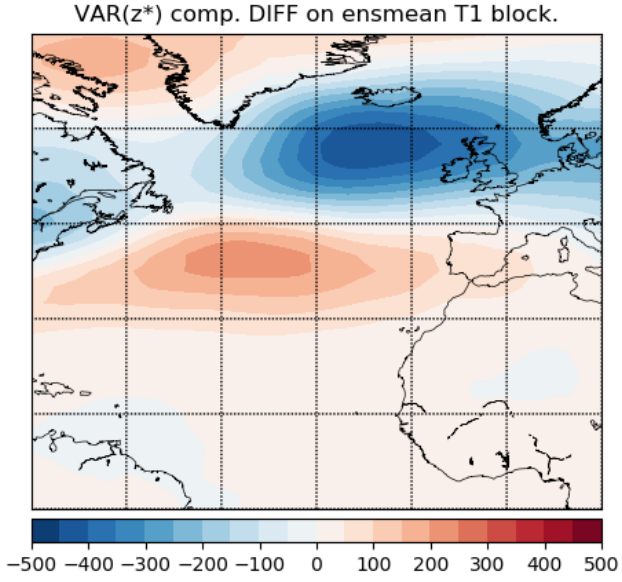

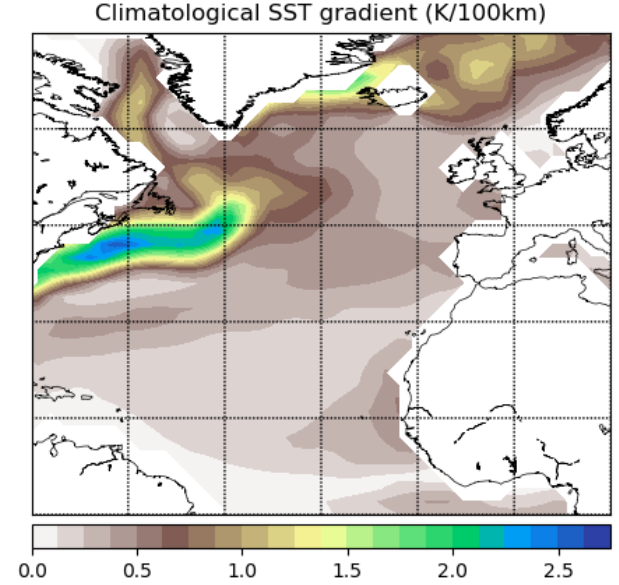

Synopsis of findings and conclusions

- Statistically significant predictive skill is found in a large ensemble of decadal hindcasts (CESM-DPLE, 40 members) for wintertime NAO and North Atlantic blocking in various lead-time ranges.

- For Greenland and Iceland blocking, the highest skill (ACC=0.58) is found at LY.1-8. At this lead-year range, the NAO exhibits comparable skill (ACC=0.59). Both of these correlations are boosted by smoothing the model timeseries. These correlations arise mainly from multi-decadal timescales.

- For Britain and Scandinavia blocking, the highest skill (ACC=0.43) is found at LY.6-7, indicating either a delayed atmospheric response, or a negative effect of the model climate drift / adjustment on its predictive skill during the first years of the forecast.

- Mapping the skill reveals coherent patches of high skill in areas of high interannual blocking variability.

- Distinct SST patterns (largely orthogonal) are associated with blocking anomalies in the two studied areas (GR-IC, BR-SC). An assessment of the origin and the limits of this predictability is ongoing.

- It is conceivable that, thanks to the large ensemble size of CESM-DPLE, predictive skill for the atmospheric circulation at the decadal time-range could emerge for the first time. These positive results call for:

  - assessing other aspects of atmospheric predictability in decadal hindcasts,
  - performing a range of sensitivity experiments to identify the associated sources of predictability,
  - increasing further ensemble sizes and using multi-model ensembles to explore the predictability limits.

References

- Athanasiadis, Wallace and Wettstein (2010): Patterns of wintertime jet stream variability and their relation to the storm tracks. J. Atmos. Sci., doi:10.1175/2009JAS3270.1.
- Athanasiadis, et al. (2014): The representation of atmospheric blocking and the associated low-frequency variability in two seasonal prediction systems. *J. Clim.*, doi:10.1175/JCLI-D-14-00291.1.
- Athanasiadis, et al. (2017): A Multisystem View of Wintertime NAO Seasonal Predictions. *J. Clim.*, doi:10.1175/JCLI-D-16-0153.1.
- Bellucci, Gualdi, Scoccimarro & Navarra (2008): NAO-ocean circulation interactions in a coupled general circulation model. Clim. Dyn., doi:10.1007/s00382-008-0408-4.
- Boer, Smith, Cassou, Doblas-Reyes et al. (2016): The Decadal Climate Prediction Project (DCPP) contribution to CMIP6. Geosci. Model Dev., doi:10.5194/gmd-9-3751-2016.
- Bretherton, Widmann, Dymnikov, Wallace & Bladé (1999): The effective number of spatial degrees of freedom of a time-varying field, *J. Clim.*, doi:10.1175/1520-0442(1999)012<1990:TENOSD>2.0.CO;2.
- Buehler, Raible & Stocker (2011): The relationship of winter season North Atlantic blocking frequencies to extreme cold or dry spells in the ERA-40. Tellus, doi:10.1111/j.1600-0870.2010.00492.x.
- Cassou (2008): Intraseasonal interaction between the Madden-Julian Oscillation and the North Atlantic Oscillation. Nature, doi:10.1038/nature07286 10.1038/nature07286
- Czaja & Frankignoul (2002): Observed impact of Atlantic SST anomalies on the North Atlantic Oscillation. J. Clim.
- Czaja & Marshall (2001): Observations of atmosphere-ocean coupling in the North Atlantic. Quart. J. R. Met. Soc.
- Davini, Hardenberg & Corti (2015): Tropical origin for the impacts of the Atlantic Multidecadal Variability on the Euro-Atlantic climate. *Env. Res. Lett.*, doi:10.1088/1748-9326/10/9/094010.
- Deser, Alexander, Xie, et al. (2010): Sea surface temperature variability: patterns and mechanisms. Ann Rev Mar Sci., 2(1), 115–143.
- Gastineau & Frankignoul (2015): Influence of the North Atlantic SST variability on the atmospheric circulation during the twentieth century. J. Clim., 28, 1396–1416.
- Häkkinen, Rhines & Worthen (2011): Atmospheric blocking and Atlantic multidecadal variability. *Science*, doi:10.1126/science.1205683.
- Hanna, Cropper, Hall & Cappelen (2016): Greenland Blocking Index 1851–2015: a regional climate change signal. Int. J. Climatol., doi:10.1002/joc.4673.

- Jianping & Wang, 2003: A New North Atlantic Oscillation Index and Its Variability, *Adv Atm Sci*, 20 (5), 661-676, doi:10.1007/BF02915394.
- Kalnay, Kanamitsu, Kistler, et al. (1996): The NCEP/NCAR 40-Year Reanalysis Project. Bull Amer Meteor Soc., 77, 437–472.
- Kushnir, et al., 2019:Towards operational predictions of the near-term climate, Nature Climate Change, 9, p.94–101, doi:10.1038/s41558-018-0359-7.
- Marshall, Kushnir, Battisti, et al. (2001): North Atlantic climate variability: phenomena, impacts and mechanisms. Intern J. Clim., 21, 1863–1898.
- Peings & Magnusdottir (2014): Forcing of the wintertime atmospheric circulation by the multidecadal fluctuations of the North Atlantic Ocean, *Env. Res. Lett.*, doi:10.1088/1748-9326/9/3/034018.
- Peng, Robinson & Li (2002): North Atlantic SST forcing of the NAO and relationships with intrinsic hemispheric variability. Geoph Res Lett., 29(8).
- Riddle, Butler, Furtado, et al. (2013): CFSv2 ensemble prediction of the wintertime Arctic Oscillation. Clim. Dyn.
- Rodwell & Rowell (1999): Oceanic forcing of the wintertime North Atlantic Oscillation and European climate. Nature, 398, 320–323.
- Sutton & Hodson (2003): Influence of the ocean on North Atlantic climate variability 1871–1999. J. Clim.
- Sutton, Norton & Jewson (2001): The North Atlantic Oscillation — What Role for the Ocean? 1, 89–100.
- Scaife, et al. (2014): Skillful long-range prediction of European and North American winters. *Geophys. Res. Lett.*, doi:10.1002/2014GL059637.
- Scherrer, Croci-Maspoli, Schwierz & Appenzeller (2006): Two-dimensional indices of atmospheric blocking and their statistical relationship with winter climate patterns in the Euro-Atlantic region. *Int J Climatol*, doi:10.1002/joc.1250.
- Wills, Armour, Battisti, et al. (2019): Ocean-atmosphere Dynamical Coupling Fundamental to the Atlantic Multidecadal Oscillation. J. Clim.
- Woollings, Hoskins, Blackburn & Berrisford (2008): A New Rossby Wave-Breaking Interpretation of the North Atlantic Oscillation. *J. Atmos. Sci.*, doi:10.1175/2007JAS2347.1.
- Woollings, Hannachi & Hoskins (2010): Variability of the North Atlantic eddy-driven jet stream. Quart. J. Roy. Meteor. Soc., doi:10.1002/qj.625.
- Yeager et al., 2018: Predicting near-term changes in the Earth system: A large ensemble of initialized decadal prediction simulations using the Community Earth System Model. *Bull. Amer. Meteor. Soc.*, doi:10.1175/BAMS-D-17-0098.1.

Thank you for your attention

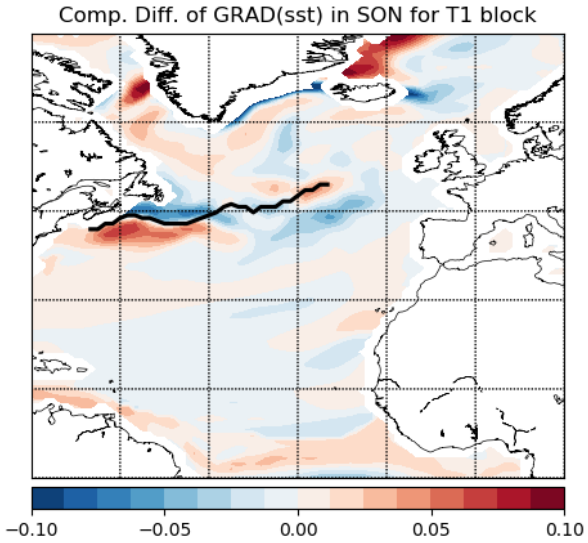

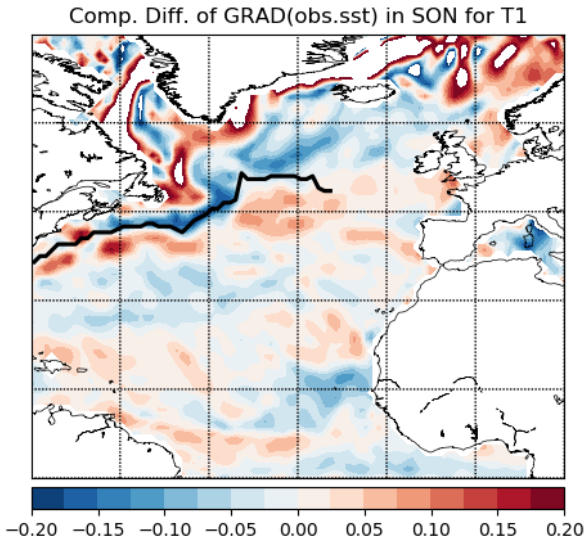

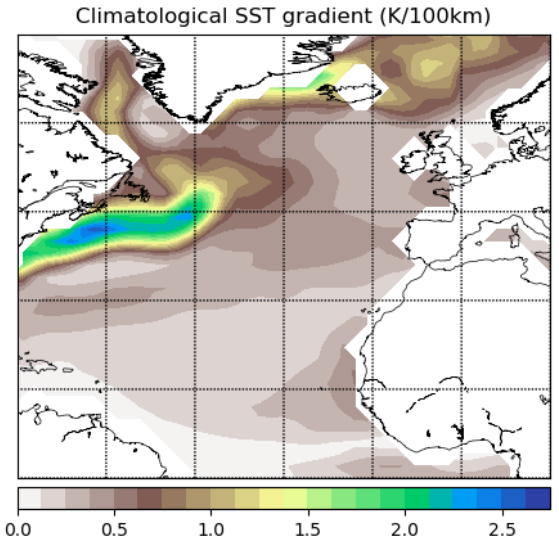

The impacts of Greenland blocking are very significant (similar to NAO).

The former include a strong feedback to the ocean via surface heat fluxes and Ekman transport anomalies forced by changes in the wind pattern [Deser et al. (2010)].

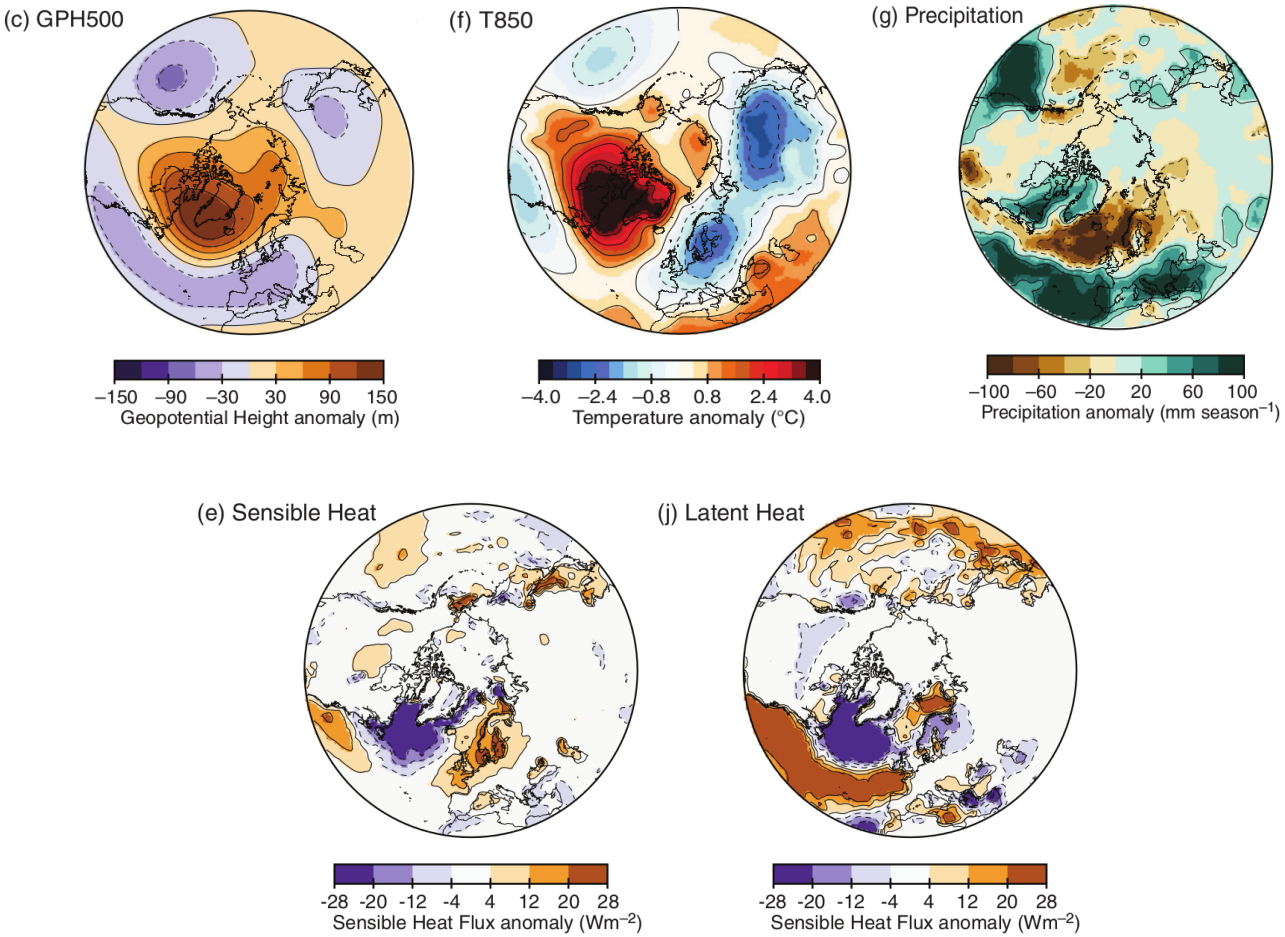

Hanna et al. (2016)

There exists extensive literature investigating the role of the ocean in forcing low-frequency (beyond interannual) atmospheric variability over the North Atlantic.

Surely, different timescales involve distinct physical forcing mechanisms and coupling (feedback closure).

Observational studies:

Marshall et al. (2001)
Czaja and Marshall (2001)
Czaja and Frankignoul (2002)
Peings and Magnusdottir (2014)
Gastineau and Frankignoul (2015)

Sensitivity experiments:

Rodwell and Rowell (1999)
Sutton, Norton and Jewson (2001)
Peng, Robinson and Li (2002)
Sutton and Hodson (2003)

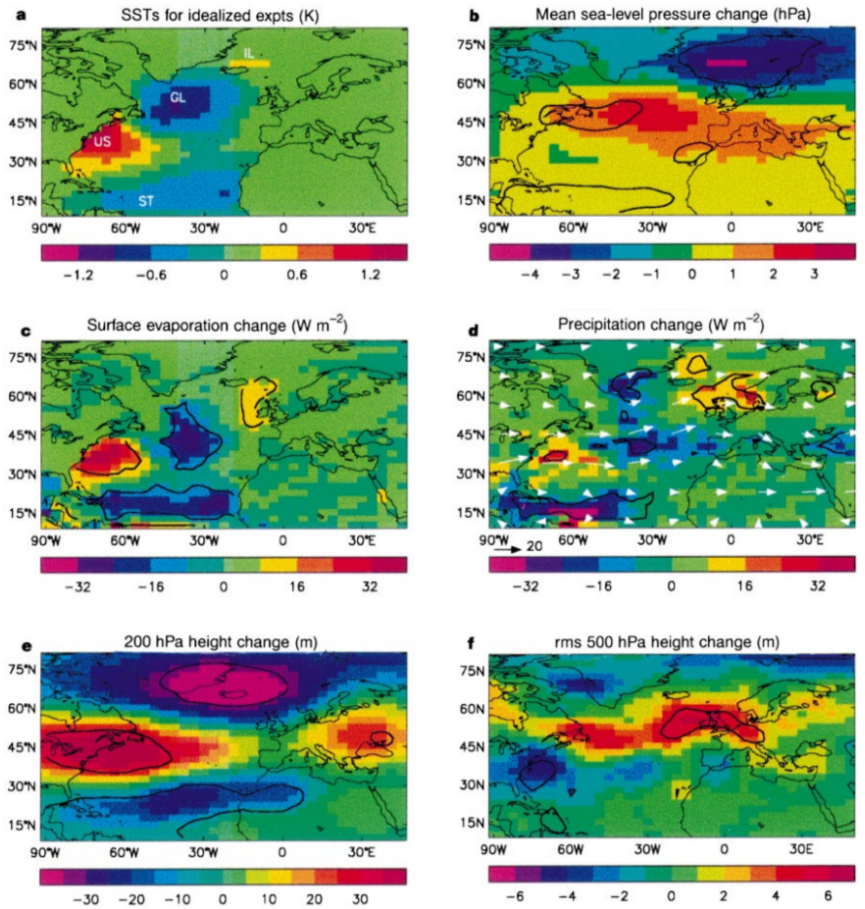

Figure 3 Model inputs and simulated responses. **a**, The pattern of SST anomalies used to force two 20-year model simulations, taken from a joint canonical correlation analysis on SSTs and MSLP[16]. The values shown correspond to the average of the monthly-varying SST anomalies used in the December to February season. For each month of the year, the scaling is calculated as two standard deviations of the time series obtained by projecting observed SSTs for that month onto the pattern. SST anomalies are added to (simulation P) or subtracted from (simulation N) a climatological SST field for 1961–90. **b**, December to February MSLP difference, simulation P minus simulation N. **c**, As **b**, but for surface evaporation in terms of latent heat flux ($W m^{-2}$). **d**, As **b** but for total precipitation in terms of condensational latent heat release ($W m^{-2}$). Superimposed are mean 500-hPa wind vectors calculated as the average of simulations P and N. The reference vector is 20 $m s^{-1}$. **e**, As **b** but for 200-hPa geopotential height. **f**, As **b** but for the 20-season mean of the r.m.s. of 2.5–6 day bandpass-filtered[27] daily 500-hPa height. In **b**–**f**, the areas within the black contours exceed the 95% confidence level of non-zero difference using a 2-tailed *t*-test.

Rodwell and Rowell (1999)

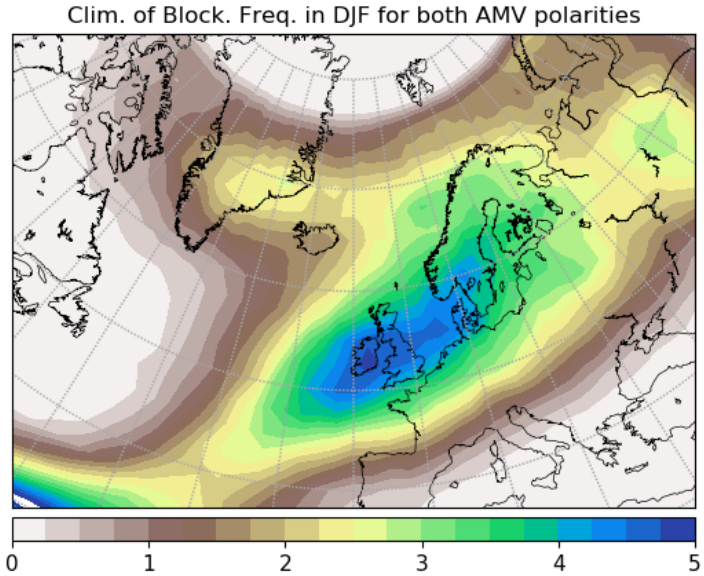

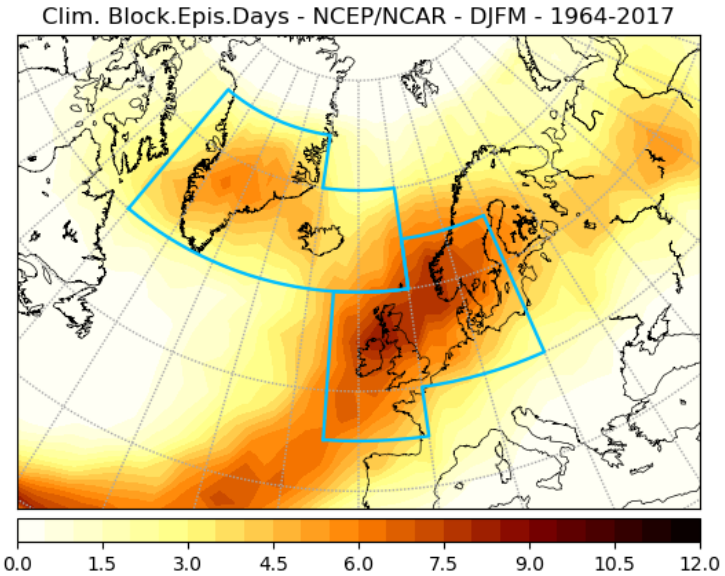

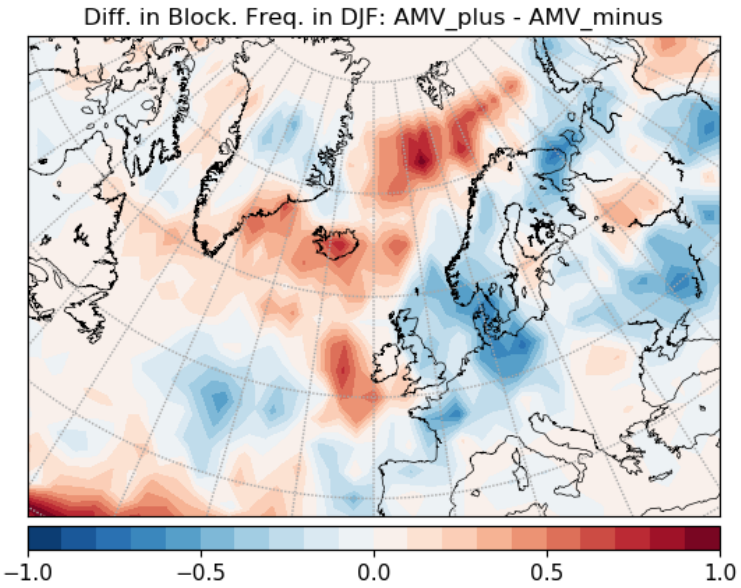

The decadal predictability found for the NAO and blocking over Greenland and Iceland may be understood as forced by oceanic dynamics, which need to be correctly initialized (AMOC anomaly). Marshall et al. (2001), Bellucci et al. (2008) and Wills et al. (2019), among others, have proposed relevant mechanisms to explain the coupled ocean—atmosphere AMV.

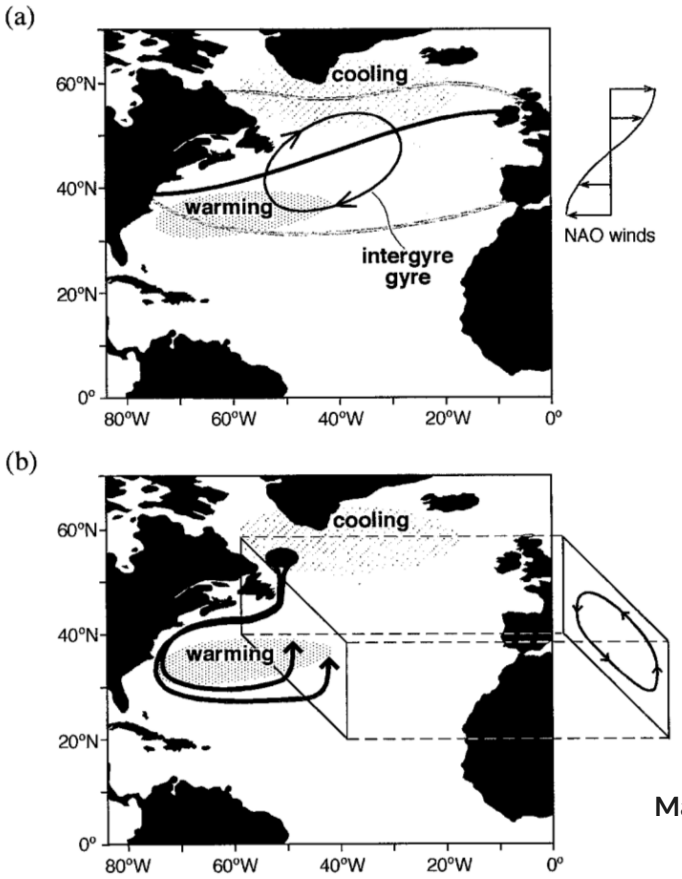

Marshall et al. (2001)

Figure 13. (a) Schematic diagram of the wind stress curl and air–sea flux anomaly patterns associated with a positive NAO. We see a 'Z' whose diagonal is the zero wind-curl line of the climatology and whose top and bottom are the zero wind-curl lines of the NAO anomaly shown in Figure 2(c). Regions of warming and cooling of the ocean due to the air–sea flux anomalies shown in Figure 2(b) are indicated. The sense of the wind-driven 'intergyre' gyre spun up by NAO(+) wind-curl forcing is also shown. (b) Schematic diagram of the anomaly in thermohaline circulation induced by the dipole in ocean thermal anomalies created by anomalies in air–sea heat fluxes associated with NAO(+) shown in Figure 2(b). The imagined anomaly in overturning circulation sketched in the meridional section on the right represents a zonal average picture

Ongoing sensitivity experiments in the framework of
the Decadal Climate Prediction Project (DCPP)

It has been suggested [e.g. Davini et al. (2015)] that the SST anomalies in the tropical Atlantic associated with the AMV are more relevant than the extratropical ones for driving the atmospheric NAO-like response, yet there is a strong indication against this proposal: CESM-LENS, although skilful in equatorial Atlantic SSTs, has no skill in GR-IC blocking and the NAO.

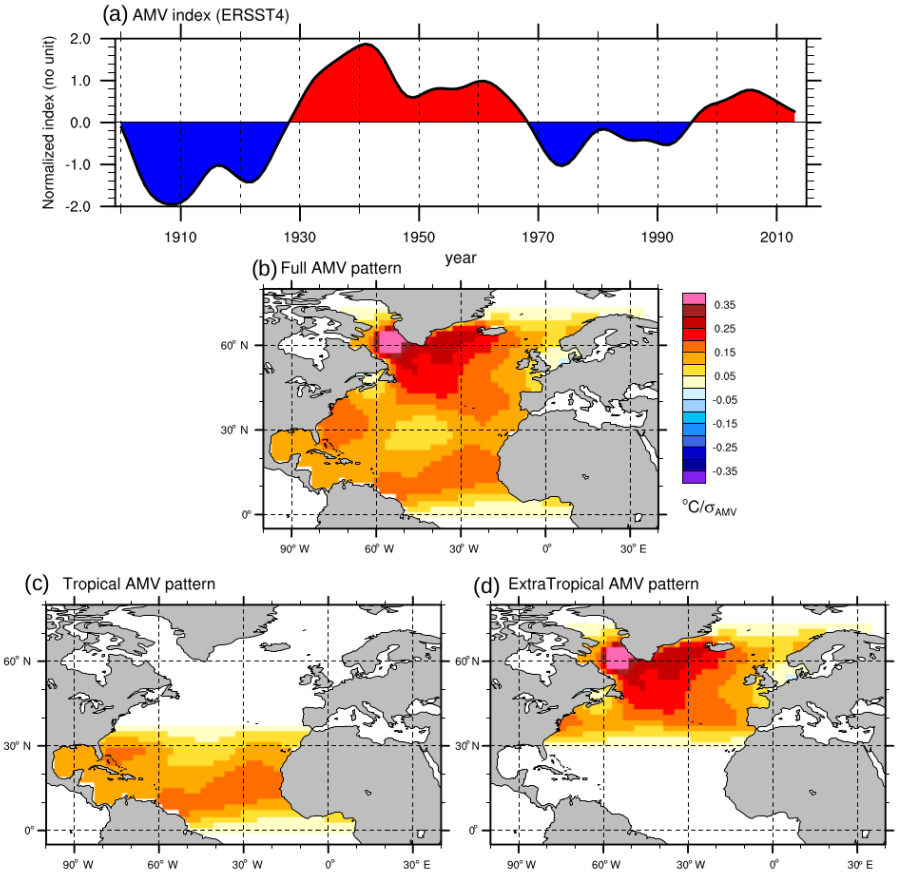

Boer et al. (2016)

Subpolar SST anomalies modulate the SST gradient at the stormtrack cyclogenesis region, consequently impacting storminess, the eddy-driven jet, NAO and Greenland blocking.

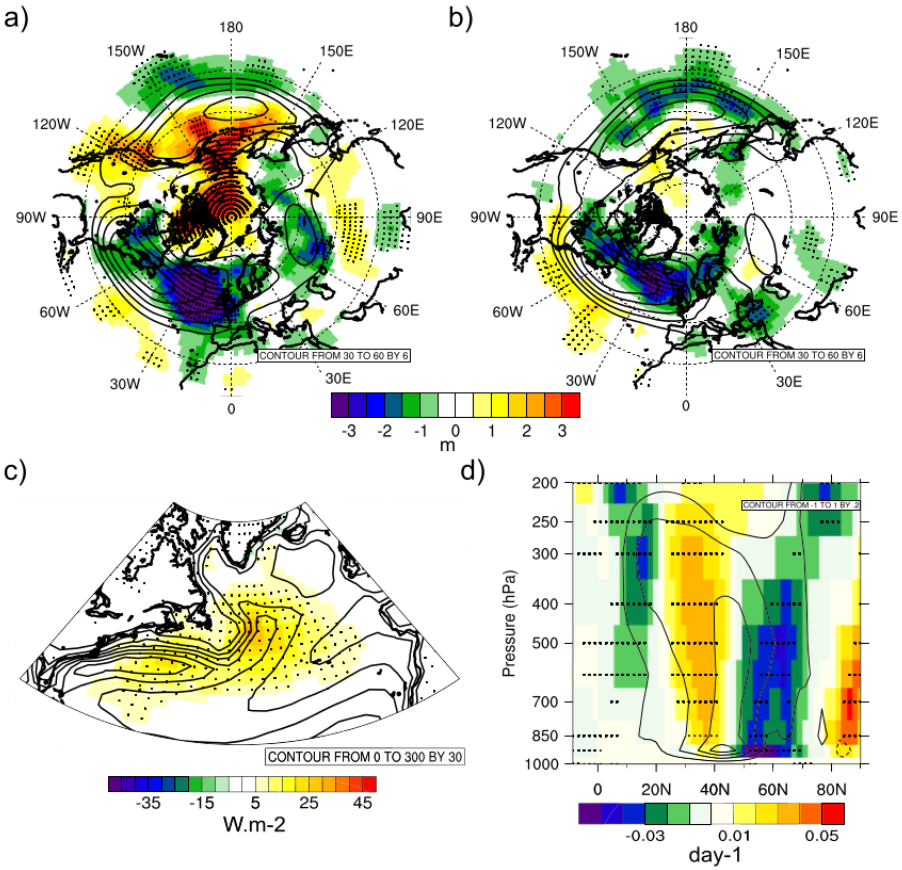

Figure 5. Physical mechanism of the atmospheric response to the AMO. (a) Winter (DJFM) transient eddy activity anomalies at 500 hPa associated with the AMO signal (57 AMO+ years minus 53 AMO− years, see list in text) in 20CR over 1901–2010 (shading in m). The climatology of transient eddy activity is shown in contours. (b) Same as (a) except for CAM5 (AMOp minus AMOn). (c) DJFM anomalies of the surface latent heat flux (shading, W m^{-2}) in CAM5 (AMOp–AMOn) and climatology in contours. (d) Pressure versus latitude plot of the DJFM Eady growth rate anomalies (day-1) over western North Atlantic (75W/30W) in CAM5 (AMOp–AMOn) and climatology in contours. Anomalies significant at the 95% level are stippled.

Peings and Magnusdottir (2014)

A multi-year positive NAO anomaly tends to strengthen the AMOC via buoyancy forcing induced by surface fluxes. The meridional heat advection associated with the AMOC anomaly finally forces a positive subpolar SST anomaly that drives [Peings & Magnusdottir (2014)] a negative NAO phase.

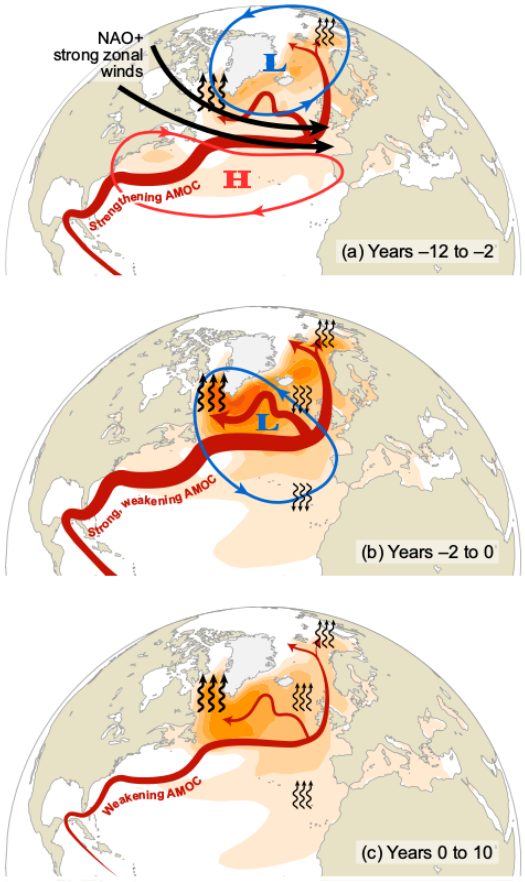

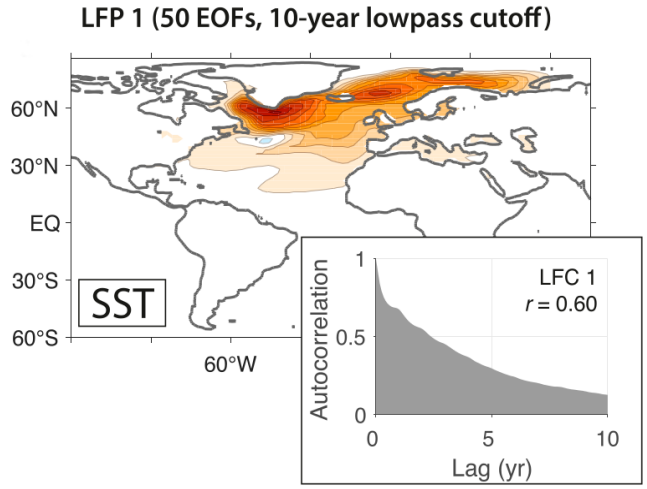

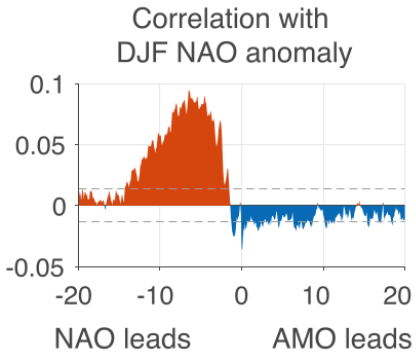

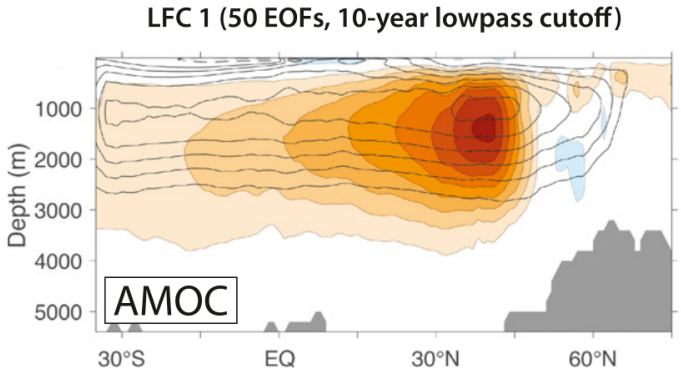

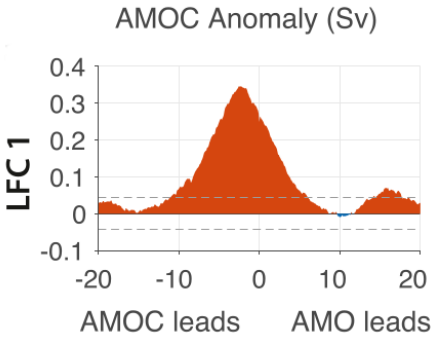

Wills et al. (2019)

In the area of the North Atlantic subpolar gyre, about half of the decadal predictive skill for SST comes from the realistic initialization, while the other half appears to come from the model dynamics (including the representation of coupled processes).

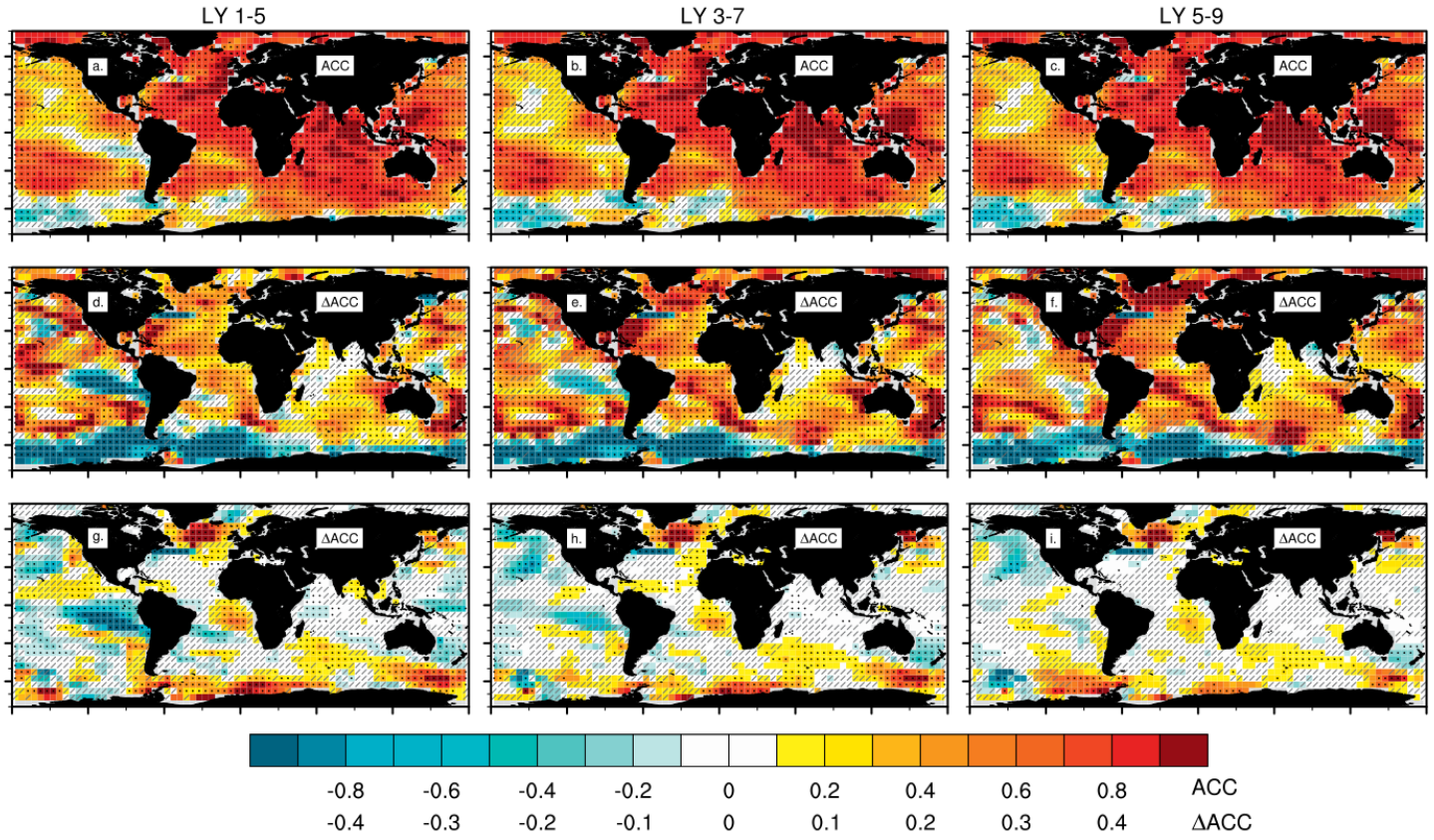

FIG. 2. (a)–(c) ACC of annual SST from CESM-DPLE relative to ERSSTv5 observations (Huang et al. 2017) for lead times of 1–5, 3–7, and 5–9 years, respectively. ACC skill score differences (d)–(f) between CESM-DPLE and persistence and (g)–(i) between CESM-DPLE and CESM-LE. All fields were mapped onto a 5° × 5° grid prior to analysis. The scale used for (d)–(i) is half that used for (a)–(c). The absence (presence) of a gray slash indicates scores that are (are not) significant at the 10% level ($\alpha = 0.1$); stippling further indicates points whose p values pass an FDR test for global (70°S–70°N) field significance ($\alpha_{global} = 0.1$).

Yeager et al. (2018)

The role of the stratosphere (a two-way interaction).

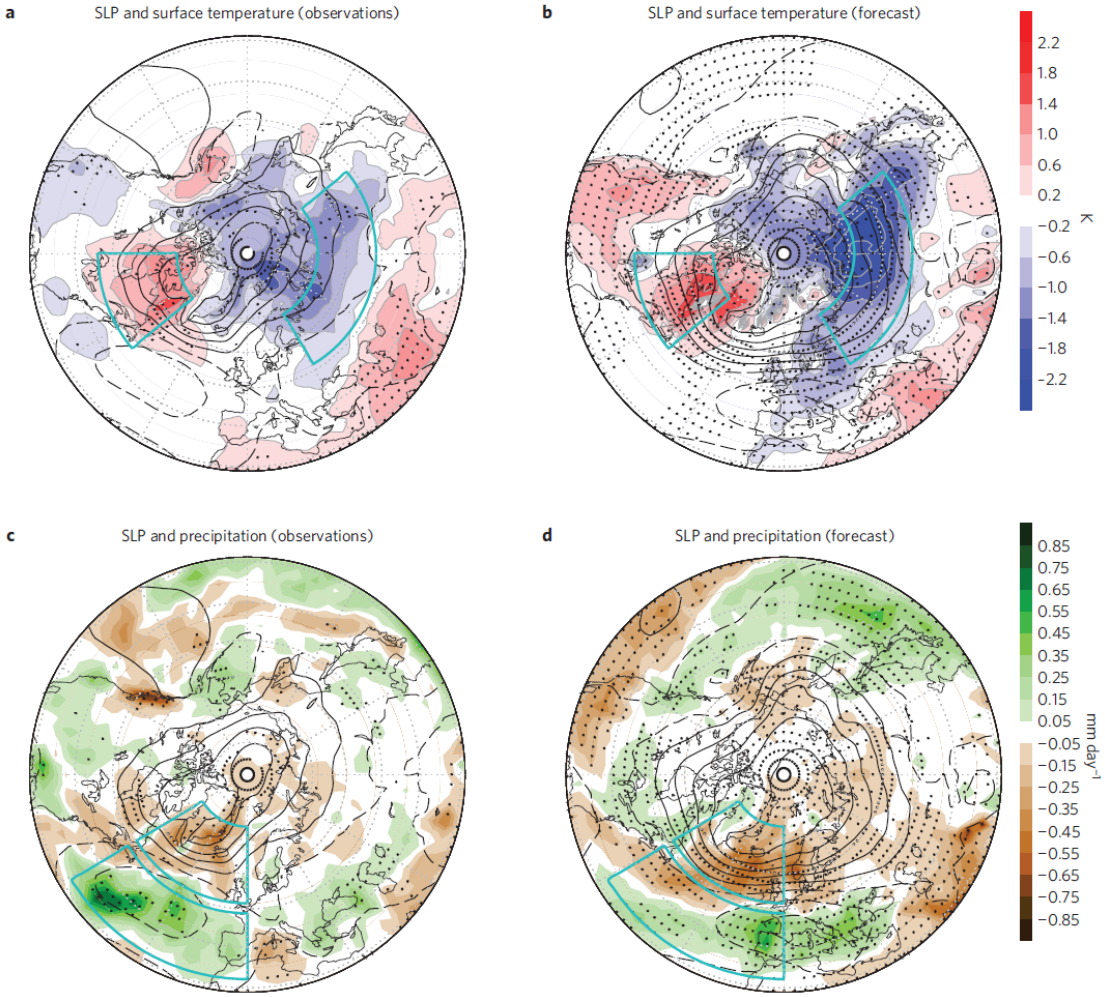

Figure 1 | Surface climate response to SSWs. a–d, Mean anomaly averaged over days 16–60 after all SSWs of SLP (contours), surface temperature (shading in **a**,**b**) and precipitation (shading in **c**,**d**) for the observations (**a**,**c**) and the model forecasts (**b**,**d**). Contour interval for SLP is 1 hPa (…, −1.5, −0.5, 0.5, …), and solid (dashed) contours denote positive (negative) values. Black dots represent statistical significance at the 90% confidence level (determined by bootstrapping) of the shaded quantities. Observed (modelled) SLP anomalies are generally significant at the 90% level where the mean anomaly exceeds ~1.5 (0.5) hPa.

Sigmont et al., Nature (2013).

The role of the oceans (also a two-way interaction).

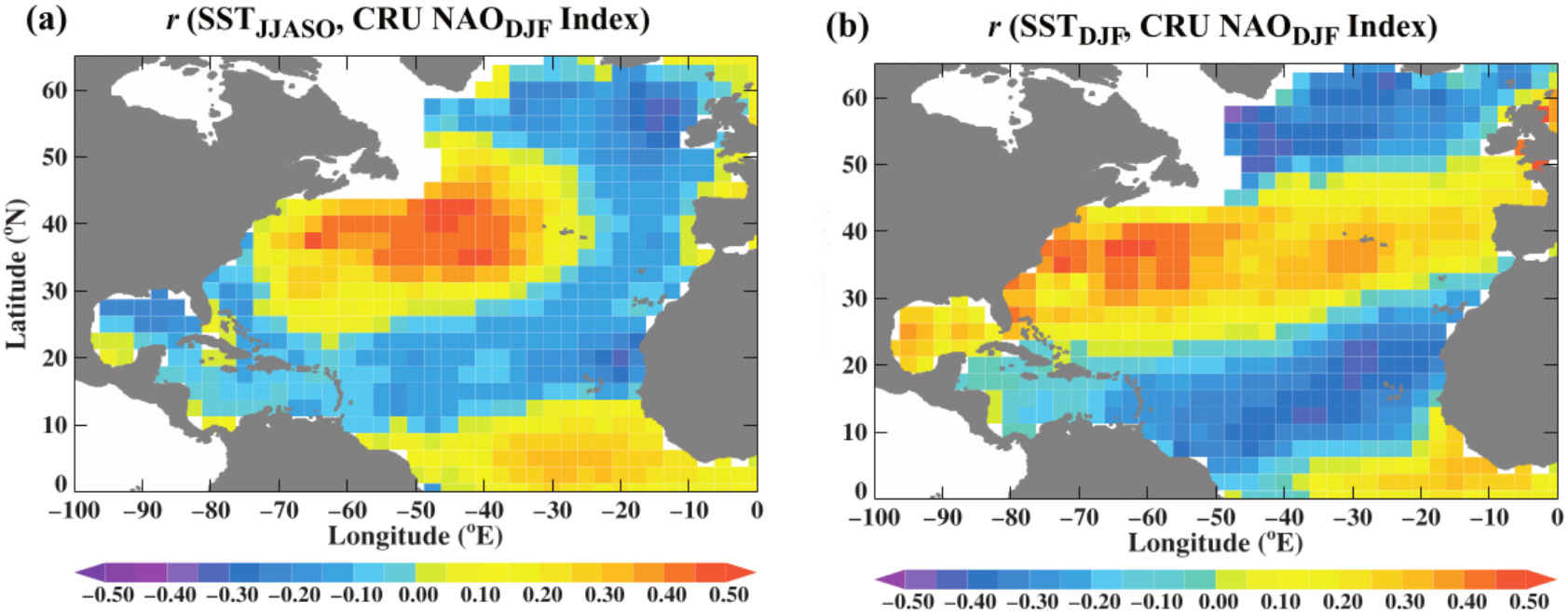

The correlation patterns of north Atlantic (a) SST_{JJASO} and (b) SST_{DJF} anomalies with the CRU NAO_{DJF} index for the period 1950/1–2000/1.

Saunders and Qian, GRL (2002).

The role of other boundary forcings (snow cover / sea-ice).

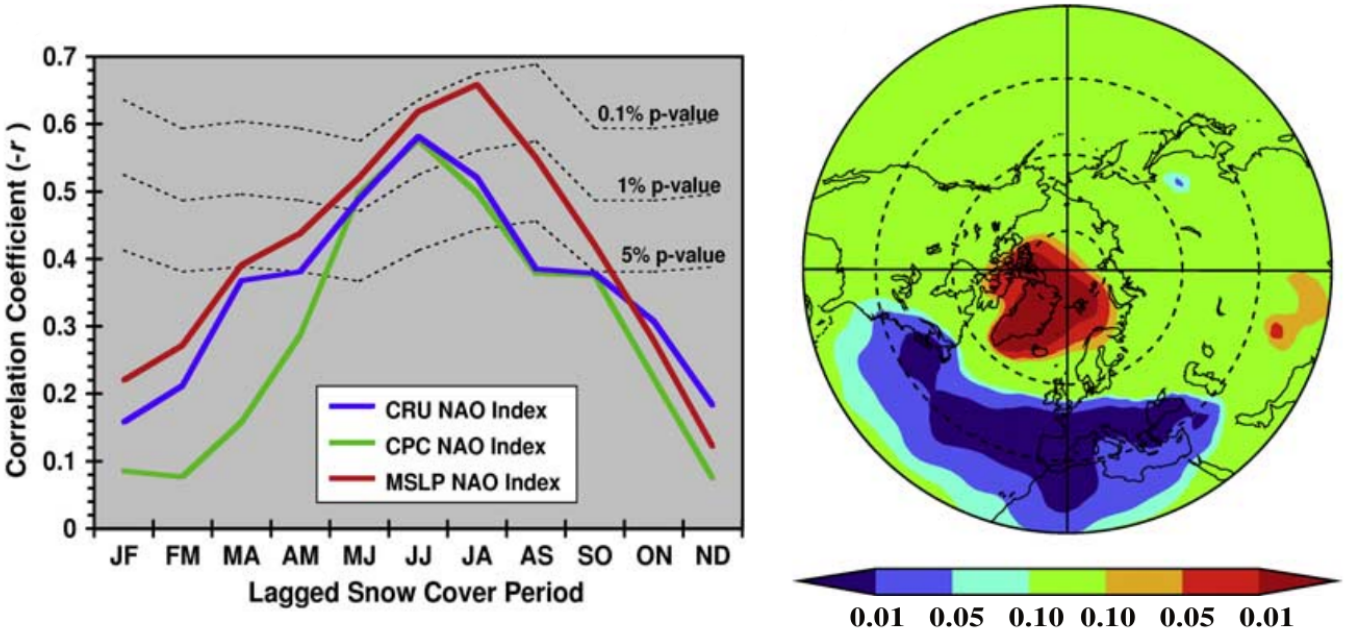

The link between summer northern hemisphere snow extent and the coming winter NAO 1972/3–2001/2. (a) The correlation between lagged northern hemisphere snow cover and winter NAO_{DJF} indices for bi-monthly snow cover periods ranging from JF (January–February) through to ND (November–December). The negative correlations from detrended time series are plotted. Dashed lines display the confidence levels of non-zero correlation between snow extent and the *MSLP NAO_{DJF} index* assessed using a 2-tailed Student's *t*-test after correction for autocorrelation with lags out to 15 years included. (b) The correlation pattern significance between detrended time series of June–July northern hemisphere snow extent and the following winter (DJF) northern hemisphere gridded sea level pressure. Significances are corrected for autocorrelation as in (a). Color shading also denotes where the correlation is either positive (orange through red) or negative (light through dark blue).

Saunders et al., GRL (2003).